

Kinetic description of a fluidized one-dimensional granular system

Rosa Ramírez* and Patricio Cordero†

Departamento de Física, Facultad de Ciencias Físicas y Matemáticas, Universidad de Chile, Santiago, Chile

(Received 15 June 1998)

In this paper we study, using Boltzmann's equation and molecular-dynamic simulations, a one-dimensional column of N inelastic point particles, in the quasielastic limit, under the influence of gravity. The column has no top boundary and it is subjected to a permanent energy injection at a fixed base chosen to behave like a "hot wall." The quasielastic condition plus the boundary condition guarantee *molecular chaos*. The energy injection is of enough intensity to keep the system permanently in a low density state. The system—which would have a homogeneous temperature if it were conservative—shows a temperature gradient because of dissipation. It is shown that, after adimensionalizing, the physical properties in the hydrodynamic limit ($N \rightarrow \infty$) depend solely on the product qN , where q is an inelasticity coefficient. Comparison of our molecular-dynamic results with this theoretical picture is excellent. [S1063-651X(99)01501-9]

PACS number(s): 81.05.Rm, 05.20.Dd, 51.10.+y, 47.50.+d

I. INTRODUCTION

Granular systems provide a number of surprising phenomena which go from gaslike to solidlike behavior [1]. Most of these phenomena imply in one way or another some degree of fluidization, and for this reason fluid states have attracted much attention in recent years [2,3]. These fluid states, however, are different from what is usually understood of fluids, and they represent a challenge and a great opportunity to look back on hydrodynamics and kinetic theory concepts [4].

Fluidization in a granular material can go from surface to total fluidization of the system. In the case of total and *dilute* fluid states, kinetic theory concepts are particularly useful when spatial and temporal correlations can be omitted from the formal description. Under such circumstances one may have the conditions for applicability of a Boltzmann equation.

To guarantee that a many-particle granular system satisfies Boltzmann's equation (mainly low density so that collisions are uncorrelated), it is necessary (a) to be in a quasielastic regime, otherwise clusters, and eventually inelastic collapse, would develop, and (b) to have a sufficiently large and permanent energy injection, to maintain a steady low density fluid state.

The energy injection needed to balance dissipation and to keep the system in a fluid state is usually implemented in practice by means of a vibrating plate. This form of energy input acts also as a source of spatial and temporal correlations, unless perhaps the injection is of enough intensity that all correlations become negligible. To avoid such a source of correlations in numerical simulations, a fixed energy source is becoming a usual practice [5–7]. Although this energy injection is not a fully realistic condition, its advantage is that the effects of the dissipative nature of the system can be isolated from those coming from a moving base.

One-dimensional models sometimes help to understand

features of specific problems (see [8] and references therein) and hopefully their properties can be extended to higher dimensions. One-dimensional granular systems share some of the phenomena of higher-dimensional systems such as transition from a condensed to a fluid state [9], inelastic collapse [10], etc., and hydrodynamic and kinetic theories have been derived for such systems basically from the associated Boltzmann equation [11,12].

In this paper we study, using the Boltzmann equation and molecular-dynamic simulations, a one-dimensional column of N inelastic point particles, in the quasielastic limit, under the influence of gravity. The column has no top boundary and it is subjected to a permanent energy injection at a fixed base chosen to behave like a "hot wall." This energy injection is of enough intensity to keep the system permanently in a low-density state. We further assume that it keeps the system in a time-independent state. This last point deserves an extra comment. There is an interesting article [6] in which the authors study a one-dimensional (1D) granular system inside a horizontal box of length L with an elastic wall and a "thermal" one. The authors report that under appropriate conditions the system stabilizes to an *oscillating state*. In our simulations we have not detected oscillations and have felt confident that time-independent solutions exist and are stable.

To prevent clustering and inelastic collapse, we will restrict ourselves to restitution coefficients r such that $(1-r)N$ is well below 1. With this last assumption and the ones described in the preceding paragraph, a Boltzmann equation is shown to be suitable to describe the system remarkably well. Even though clustering is an important phenomenon, its presence would invalidate the use of Boltzmann's equation. There is a wide zone in phase space, though, where the presence of clusters can be neglected [13,14].

Work has already been done to derive a distribution function for a granular 1D gas in the quasielastic limit. In [7,11] the authors find distribution functions for a column of inelastic particles without gravity. In [15] the authors find a set of equations for a similar system subjected to gravity, that can be solved numerically to find the distribution function.

*Electronic address: roramire@cec.uchile.cl

†URL: www.cec.uchile.cl/cinetica/

In this paper, starting with a Boltzmann equation including the effects of the inelastic collisions and using the quasi-elastic and ($N \rightarrow \infty$) limit, we find the analytic perturbative solution for the system. We will show that these solutions depend on the parameter $(1-r)N$ alone except for a scale factor that emerges after adimensionalizing the problem. Our solution is not comparable to [15] because they use an asymmetric sawtooth moving base, which causes the density to increase with increasing height. In our system, and because we use a thermal boundary condition and no top wall, density decreases with height.

Dissipative collisions give rise to a heat flux and a temperature profile with a negative gradient, even in the quasi-elastic limit. We show that a perturbative expansion of the distribution function predicts correctly these effects for small $(1-r)N$ values. The validity of our theoretical results—in particular, our predictions for the values of the moments of the distribution function—are then compared with our own simulational results obtained from event-driven molecular dynamic simulations.

This paper introduces Boltzmann's equation with dissipation in Sec. II, develops and uses a perturbative scheme in Sec. III, and makes a comparison between theory and results from simulations in Sec. IV. Final comments are in Sec. V.

II. THE MODEL AND BOLTZMANN'S EQUATION

A. The system

We examine the behavior of N identical point particles under the action of gravity, a fixed base, and no top boundary. The collisions between particles, $(c_1, c_2) \rightarrow (c_1', c_2')$, are inelastic,

$$c_1' = qc_1 + (1-q)c_2, \quad c_2' = qc_2 + (1-q)c_1, \quad (1)$$

where $0 \leq q \leq 1/2$, and $q=0$ corresponds the perfectly conservative case. The usual restitution coefficient is $r=1-2q$.

Let us briefly comment that if we relabel particles after each collision, so that in Eq. (1) $c_1' \leftrightarrow c_2'$, then it is seen that the limit q small and different from zero is tantamount to a system of N point particles that pass through each other without ever interacting. In the case $q \neq 0$, particles pass through each other losing some energy in the process as if moving in a viscous background. It is quite important to underline the relevance of this picture to the *molecular chaos hypothesis* needed to justify the use of Boltzmann's equation. Since two colliding particles [call them (a, b)] pass through each other altering their velocities, they pass through all the rest of the particles before meeting again. In fact, for them to be about to collide, again a has passed through N_a particles, b through N_b particles, and $N_a + N_b = N - 2$. For a large enough system this is enough for particles to decorrelate their velocities. In the case of the boundary condition that we are about to define, the situation is even more extreme because either a or b will necessarily hit the base (forgetting its history altogether) before encountering its partner again. In our case, then, the velocities of particles about to collide are uncorrelated.

A permanent energy injection, needed to keep the system in a fluid state, enters through the fixed base as if it were a "hot wall." A particle hitting the base with velocity c' in-

stantaneously bounces back with a velocity c taken from a probability $W(c)$, uncorrelated from the incoming velocity c' . The formalism developed in this paper can be extended to a generic $W(c)$ but in what follows we have chosen the "thermal" probability,

$$W(c) = \frac{2c}{\alpha^2} e^{-c^2/\alpha^2}, \quad (2)$$

where α is a parameter with dimensions of velocity that characterizes the "temperature" of the base.

Different fixed-base probabilities W have been discussed in [5,7], while in [16] the correlated probability $W(c, c')$ is derived for a sawtooth vibrating plate. Even though it is less realistic than a vibrating condition, the "thermal" boundary condition has the advantage of isolating the effects of the dissipative nature of the system from those coming from a moving base. Furthermore, it is analytically simpler to impose in the formalism and it is easy to implement in a molecular-dynamic program.

Let us see that the "hot-wall" boundary condition is not totally unrealistic. A vibrating base has a frequency ω and an amplitude A . A control parameter much used in this context is $\Gamma = A\omega^2/g$. Consider the case of an amplitude much smaller than the mean free path near the base and a frequency much larger than the collision rate with the base and yet with Γ finite. Such a base is almost at a fixed position but injecting as much energy as desired since it is fixed with Γ . Warr and Huntley in [2] have shown that a free particle hitting quasielastically a vibrating bed produces an outgoing velocity distribution which, to first order, is a Gaussian.

B. Kinetic equation and boundary condition

The standard form for the one-dimensional and time-independent Boltzmann equation for the distribution function $f(x, c)$ normalized to

$$\int dx \int dc f(x, c) = 1, \quad (3)$$

for particles that interact with the collision rule (1), is

$$\left(c \frac{\partial}{\partial x} - g \frac{\partial}{\partial c} \right) f(x, c) = N \int_{-\infty}^{\infty} \left[\frac{1}{(1-2q)^2} f(x, c_1'', t) f(x, c_2'', t) - f(x, c_1, t) f(x, c_2, t) \right] |c_2 - c_1| dc_2, \quad (4)$$

where the double-prime variables are associated to the inverse collisions, $c_1'' = [(1-q)c_2 - qc_1]/(1-2q)$, $c_2'' = [(1-q)c_1 - qc_2]/(1-2q)$. It can be shown that the precise generic factor, which in Eq. (4) is $1/(1-2q)^2$, for any type of instantaneous one-dimensional two-particle hard collision rule is $|c_2'' - c_1''|/|c_2 - c_1|J$, where $J(c'', c)$ is the Jacobian of the transformation $(c_1'', c_2'') \rightarrow (c_1, c_2)$.

Equation (4) can be formally expanded in powers of q , and it has been shown to yield [12]

$$\left(c \frac{\partial}{\partial x} - g \frac{\partial}{\partial c}\right) f(x, c) = N \sum_{k=1}^{\infty} \frac{q^k}{k!} \frac{\partial^k}{\partial c^k} (M^{(k)}(x, c) f(x, c)), \quad (5)$$

where the moments $M^{(k)}(x, c)$ are

$$M^{(k)}(x, c) = \int_{-\infty}^{\infty} f(x, c') (c - c')^k |c - c'| dc'. \quad (6)$$

The right-hand side of Eq. (5) is identically zero for the perfectly elastic limit ($q=0$), as it should be. Only when considering correlations and the finite size of the particles (as in Enskog's equation) would the right-hand side of the kinetic equation be nontrivial in the elastic limit.

We rewrite Eq. (5) taking the product qN as a single parameter,

$$\left(c \frac{\partial}{\partial x} - g \frac{\partial}{\partial c}\right) f(x, c) = \sum_{k=1}^{\infty} \frac{(qN)^k}{k! N^{k-1}} \frac{\partial^k}{\partial c^k} (M^{(k)}(x, c) f(x, c)). \quad (7)$$

From this last equation it is seen that in the $N \rightarrow \infty$ limit (*hydrodynamic limit* from now on) with qN finite, only the first term of the last expansion survives in the kinetic equation, and this becomes

$$\left(c \frac{\partial}{\partial x} - g \frac{\partial}{\partial c}\right) f(x, c) = qN \frac{\partial}{\partial c} (M^{(1)}(x, c) f(x, c)). \quad (8)$$

This equation corresponds to the hydrodynamic and quasi-elastic limit. A nice physical derivation of a similar equation is in [12]. Briefly, Eq. (8) statistically represents a particle passing through a viscous fluid losing energy and consequently suffering an acceleration $-(g + qNM^{(1)})$.

Any solution $f(x, c)$ of Eq. (8) must satisfy the thermal condition at the base. The boundary condition for an uncorrelated probability $W(c)$ can be written in the form [17]

$$|c| f(0, c > 0) = KW(c) \quad (9)$$

with

$$K = \int_{-\infty}^0 f(0, c') |c'| dc',$$

where K is the collision rate with the base, and the function $W(c)$ satisfies $\int_0^{\infty} W(c) dc = 1$. The probability (2) introduces the ‘‘temperature’’ $\alpha^2/2$ and we remark that, if the system were perfectly elastic, this would be the homogeneous temperature of the system.

C. Adimensionalization of the problem

Having introduced the ‘‘temperature’’ at the base, we define the reduced variables X, C , a distribution function $F(X, C)$, and the moment $\hat{M}^{(1)}(X, C)$ such that $x = \alpha^2 X / (2g)$, $c = \alpha C$, $f(x, c) = 2g F(X, C) / \alpha^3$, $M^{(1)}(x, c) = 2g \hat{M}^{(1)}(X, C)$. Equation (8) becomes

$$\left(C \frac{\partial}{\partial X} - \frac{1}{2} \frac{\partial}{\partial C}\right) F(X, C) = qN \frac{\partial}{\partial C} (\hat{M}^{(1)}(X, C) F(X, C)). \quad (10)$$

By further defining $w(C) = \alpha W(c)$ and $k = \alpha K / (2g)$ still with $\int_0^{\infty} w(C) dC = 1$, the boundary condition at the base becomes $|C| F(0, C > 0) = kw(C)$ with $k = \int_{-\infty}^0 F(0, C) |C| dC$. Our specific choice then is $w(C) = 2C e^{-C^2}$.

As we see, the only parameter left in the adimensional formalism is qN . There is no tunable parameter like gravity or the temperature imposed at the base. Hence, except for a scale factor, the quasielastic system is completely determined by qN alone.

III. PERTURBATIVE SOLUTION

A. The s -order equation and associated boundary condition

To solve Eq. (10) we assume that $F(X, C)$ can be formally expanded in powers of qN ,

$$F(X, C) = \sum_{s=0}^{\infty} (qN)^s F_s(X, C). \quad (11)$$

In order to have a first-order correction much smaller than the zeroth-order distribution function, we require that qN be distinctly smaller than 1. From Eqs. (10) and (11), a hierarchy of equations follows:

$$\left(C \frac{\partial}{\partial X} - \frac{1}{2} \frac{\partial}{\partial C}\right) F_s(X, C) = \sum_{n=0}^{s-1} \frac{\partial}{\partial C} (\hat{M}_n^{(1)}(X, C) \times F_{s-n-1}(X, C)), \quad (12)$$

where we have defined s -order moments $\hat{M}_s^{(k)}(X, C)$ as

$$\hat{M}_s^{(k)}(X, C) = \int_{-\infty}^{\infty} (C - C')^k |C - C'| F_s(X, C') dC'. \quad (13)$$

At each order s in Eq. (12), the unknown function F_s appears only on the left-hand side of the equation while the right-hand side contains functions F_r with $r < s$. The integration of the set of equations (12), therefore, is straightforward. We impose the normalization condition (3) in the form $\int_0^{\infty} dX \int_{-\infty}^{\infty} dC F_s(X, C) = \delta_{0s}$. It is easy to prove that $\hat{M}_s^{(1)}(X, C)$ obeys $(\partial_C) \hat{M}_s^{(1)} = 2\hat{M}_s^{(0)}$ and therefore the equations for the first three functions F_s become

$$\left(C \frac{\partial}{\partial X} - \frac{1}{2} \frac{\partial}{\partial C}\right) F_0 = 0, \quad (14)$$

$$\left(C \frac{\partial}{\partial X} - \frac{1}{2} \frac{\partial}{\partial C}\right) F_1 = \left(2\hat{M}_0^{(0)} + \hat{M}_0^{(1)} \frac{\partial}{\partial C}\right) F_0, \quad (15)$$

$$\left(C \frac{\partial}{\partial X} - \frac{1}{2} \frac{\partial}{\partial C}\right) F_2 = \left(2\hat{M}_0^{(0)} + \hat{M}_0^{(1)} \frac{\partial}{\partial C}\right) F_1 + \left(2\hat{M}_1^{(0)} + \hat{M}_1^{(1)} \frac{\partial}{\partial C}\right) F_0. \quad (16)$$

Any of these F_s functions must obey a normalization [see Eq. (19) below] and the boundary condition $|C|F_s(0,C>0) = k_s w(C)$ with a suitable k_s constant [see Eq. (20) below].

It will be seen that for about $qN \leq 0.01$ the behavior of the system is well described expanding up to first order, while for $0.01 \leq qN \leq 0.1$ the second-order correction is needed. In the following we describe the method to get these two corrections for our system.

The equation for F_0 is the only equation in the case of the conservative system ($q=0$) and in our case it corresponds to a fixed temperature system subjected to gravity. More on this will be in Sec. III C.

B. The energy as a variable

The differential operator ($C\partial_X - 1/2\partial_C$), present in all the equations, suggests that the energy variable

$$\tau = X + C^2 \quad (17)$$

will play a privileged role. For example, any differential function of τ alone satisfies Eq. (14). We would like to point out that

$$\tau = \frac{mgx + mc^2/2}{k_B T_0}, \quad (18)$$

if the identification $\alpha = \sqrt{2k_B T_0/m}$ is made, k_B is the Boltzmann constant, T_0 is the temperature at the base, and m is the mass of each particle. From this point of view τ resembles a Froude number in the sense that it is a ratio between two energies, but it is not a fixed parameter in one ‘‘experiment’’ but rather an alternative phase-space variable. For this reason we refer to it simply as an adimensional energy variable.

$$\Phi_s(\tau, C) = 2 \int_C^{\sqrt{\tau}} [\text{right-hand side of Eqs. (14)–(16)}](\tau, C') dC' + B_s(\tau), \quad (21)$$

where $B_s(\tau)$ is an integration constant. The boundary condition (20) is a condition over $\Phi_s(\tau, \sqrt{\tau})$, namely, the lower limit in the integral above equals the upper limit and therefore the boundary condition is simply

$$B_s(\tau) = k_s \frac{w(\sqrt{\tau})}{\sqrt{\tau}}, \quad (22)$$

where the constant k_s is determined from the normalization condition (19).

C. The zeroth-order solution

A generic solution of Eq. (14) is any function of τ alone but from the boundary condition it follows that

$$\Phi_0(\tau) = \frac{w(\sqrt{\tau})}{2\sqrt{\pi\tau}} = \frac{1}{\sqrt{\pi}} e^{-\tau} = \frac{1}{\sqrt{\pi}} e^{-X-C^2}. \quad (23)$$

The new variables replacing (X, C) will be (τ, C) , the Jacobian being 1. When the distribution is written in terms of them, it will be denoted $\Phi(\tau, C) = F(\tau - C^2, C)$ and the moments $\bar{M}^{(k)}(\tau, C) = \hat{M}^{(k)}(\tau - C^2, C)$.

The normalization condition, using (τ, C) as independent variables, can be written in two forms,

$$\delta_{0s} = \int_0^\infty d\tau \int_{-\sqrt{\tau}}^{\sqrt{\tau}} dC \Phi_s(\tau, C) = \int_{-\infty}^\infty dC \int_{C^2}^\infty d\tau \Phi_s(\tau, C) \quad (19)$$

while the boundary condition for each of the Φ_s is, provided that $C = \sqrt{\tau}$ when $X=0$,

$$\sqrt{\tau} \Phi_s(\tau, \sqrt{\tau}) = k_s w(\sqrt{\tau}) \quad (20)$$

with

$$k_s = \int_{-\infty}^0 \Phi_s(C^2, C) |C| dC.$$

The variables (τ, C) and the functions Φ_s are the most convenient quantities to solve the problem and write down the solution, but when it comes to discussing the physics of the problem or to evaluating the hydrodynamic fields, we continue using (X, C) and the functions F_s .

In terms of the new variables (τ, C) , the differential operator ($C\partial_X - 1/2\partial_C$) that appears on the left-hand side of the kinetic equations gets substituted by $(-1/2)\partial/\partial C$. Hence these equations are solved simply integrating the right-hand side of Eqs. (14)–(16) over C with τ fixed. In practice what we do is

This is the exact solution in the conservative case ($q=0$) and it corresponds to a Boltzmann distribution with a homogeneous temperature and with an associated number density that decreases exponentially with height. Had we chosen a different boundary condition, the temperature would not be perfectly homogeneous in the elastic case. This is one of the advantages of choosing the thermal boundary condition from other possible ones, namely, the effects of dissipation described below are seen more clearly.

Since F_0 is an even function of C , it follows that the functions $\bar{M}_0^{(k)}$ have parity $(-1)^k$ with respect to inverting C . The ones we will use to solve the first-order correction can be expressed analytically,

$$\bar{M}_0^{(0)}(\tau, C) = \frac{1}{\sqrt{\pi}} e^{-\tau} [\sqrt{\pi} \operatorname{erf}(C) C e^{C^2} + 1], \quad (24)$$

$$\bar{M}_0^{(1)}(\tau, C) = \frac{1}{\sqrt{\pi}} e^{-\tau} [\sqrt{\pi} \operatorname{erf}(C) (C^2 + \frac{1}{2}) e^{C^2} + C]. \quad (25)$$

D. The first-order correction

The first-order equation (15) in terms of (τ, C) is

$$-\frac{1}{4} \frac{\partial \Phi_1}{\partial C} = \left[C \bar{M}_0^{(1)} \frac{\partial}{\partial \tau} + \bar{M}_0^{(0)} \right] \Phi_0(\tau). \quad (26)$$

Since the right-hand side of this equation is even in C , it is possible to split the solution in the form $\Phi_1 = \Phi_1^{\text{odd}} + \Phi_1^{\text{even}}$ and the even piece cannot depend on C . Following the prescriptions (21) and (22) and making use of the normalization condition leads to

$$\Phi_1^{\text{odd}}(\tau, C) = \frac{2}{\pi^{3/2}} e^{-2\tau} \left\{ \sqrt{\pi} C - \pi \operatorname{erf}(C) \left(\frac{3}{2} - C^2 \right) e^{C^2} \right\}, \quad (27)$$

$$\Phi_1^{\text{even}}(\tau) = \frac{2}{\pi^{3/2}} e^{-\tau} \left\{ 1 + \pi \operatorname{erf}(\sqrt{\tau}) \left(\frac{3}{2} - \tau \right) - \sqrt{\pi \tau} e^{-\tau} \right\}. \quad (28)$$

From these functions the corrections $F_1^{\text{odd}}(X, C)$ and $F_1^{\text{even}}(X, C)$ are naturally defined.

It can be checked that the hydrodynamic velocity to first order at any point X vanishes as expected. The solution up to first order predicts, near the base, a density larger than the density for the conservative case. It also predicts a negative temperature gradient and an upwards heat flux. The even moments of the distribution, such as the number density $n(X)$ or the pressure, cannot be expressed analytically in a close form, but they have been calculated numerically and the results are shown in the next section.

Remarkably the upwards heat flux J_Q has an *analytic* expression. J_Q corresponds to the flux of the energy being dissipated in the bulk. Taking into account that the distribution function is normalized to 1, the following expression is the heat flux per particle:

$$J_Q(X) = qN \int_{-\infty}^{\infty} dC \frac{C^3}{2} F_1^{\text{odd}}(X, C) = \frac{qN}{\sqrt{2\pi}} e^{-2X}. \quad (29)$$

At the top, Fig. 1 shows F_1 evaluated at three different heights. It is seen that, at $X=0$, $F_1(0, C)$ has a discontinuous derivative at $C=0$, which, from a mathematical point of view, can be understood because F_1^{even} is an analytic function of the positive variable $\sqrt{X+C^2}$ which at $X=0$ is $|C|$. Physically, the singular behavior of the distribution is understood because the particles with $C>0$ close to the base have basically a Boltzmann distribution since most of them have just hit the base losing their memory, while the particles about to hit the base carry the ‘‘dissipative’’ information from the bulk. These two distribution functions have quite a different origin and they meet at $(X=0, C=0)$.

Going to higher X values, wall effects diminish, and the system tends to behave ‘‘isotropically’’ in the bulk, as one would expect. Notice that the ratio $\Phi_1^{\text{odd}}/\Phi_1^{\text{even}}$ decays exponentially as $e^{-\tau} = e^{-X-C^2}$, namely, away from the base the first-order correction becomes more and more symmetric in C .

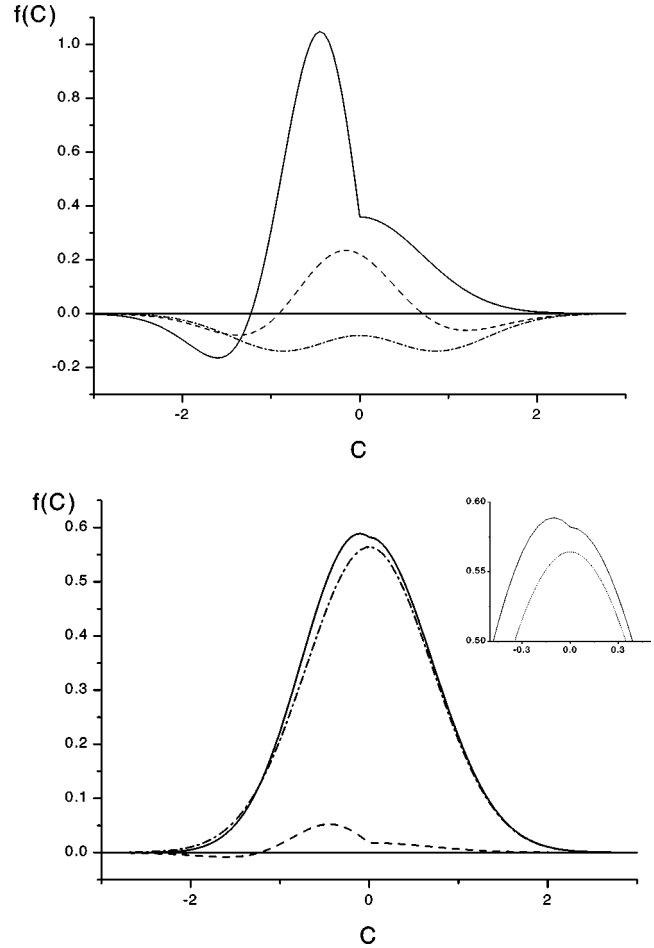


FIG. 1. At top F_1 is shown at different heights: $X=0$ (solid line), $X=1$ (dashed line), and $X=2$ (dot-dashed line). The function tends to be more symmetric with height. At bottom the distributions F_0 (dot-dash line) and $F_0 + (qN)F_1$ (solid line) evaluated at the base ($X=0$) are compared when $qN=0.05$. The function $(qN)F_1$ (dashed line) is also included. The inset shows the detail of the distribution about $C=0$.

At bottom, in Fig. 1, F_0 is compared with $F = F_0 + qNF_1$ at $X=0$ for $qN=0.05$. The function qNF_1 has also been included.

As an effect of the dissipative dynamics, the system obviously cools down. This effect is not symmetric and it implies, as we discuss later on, that particles going up move faster, on the average, than particles coming down.

Particles falling through a viscous fluid have a speed limit. The meaning of the maximum that the velocity distribution at $X=0$ shows for negative velocities seems to be related to a similar phenomenon even though our fluid cannot be described like a uniform viscosity fluid.

It can also be seen and checked numerically that qNF_1 becomes comparable to and even larger than F_0 for negative enough velocities. Since the complete distribution F is positive, this is an indication that the contribution of large negative velocities is not well described at this order but the relevance of this inaccuracy to the general description of the system is marginal.

Finally we remark that far from the base (large X) the density is quite small, the mean free path of particles is com-

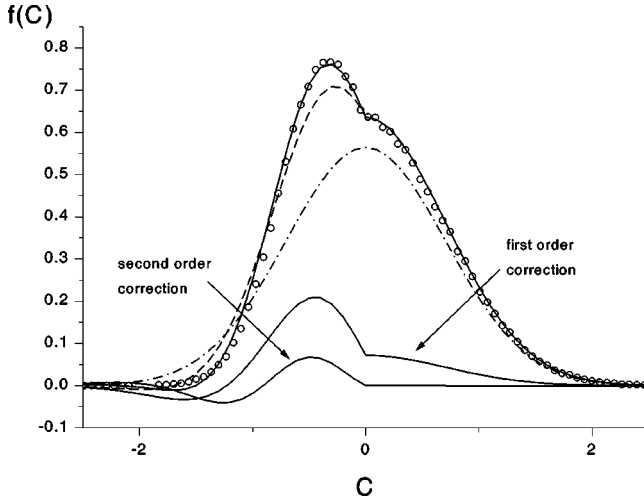


FIG. 2. The distribution functions normalized to 1 at $X=0$ evaluated to zeroth (dot-dashed line), first (dashed line), and second order (solid line) are seen in this figure for $qN=0.2$ and $N=200$. The distribution up to second order differs by more than 30% from F_0 in the central region and, in spite of this, the former fits extraordinarily well the observed distribution (open circles). The solid S-shaped curves underneath represent the first- and second-order corrections, $(qN)F_1$ and $(qN)^2F_2$. Notice that the last correction is almost zero for positive velocities.

parable to the size of the system, and the first-order correction function qNF_1 is no longer small compared to F_0 .

E. The second order correction

The function F_2 can formally be integrated, following the prescription (21), as we did to obtain F_1 except that some of the integrals cannot be written explicitly in a closed form. Those integrals have been evaluated using a standard Monte Carlo method.

In Fig. 2 the theoretical distribution functions up to zeroth, first, and second order evaluated at $X=0$ with $qN=0.2$ are compared with the measured distribution function. Although $qN=0.2$ is quite high for our formalism, we have chosen this value to show how well the theory fits the observations. This figure also shows $(qN)^2F_2$. As can be observed, this last function is practically zero for positive velocities, whereas for the negative ones it removes high velocity particles and adds slow ones. This happens because the dissipative effects influence much more the stream of particles coming down—after having suffered many collisions—than their counterparts going up.

The maximum that the distribution has for negative velocities is reinforced by the second-order correction. We have determined that it corresponds to about

$$C_{\max} \approx -qN(2.5 - 4.3qN). \quad (30)$$

IV. COMPARISON WITH SIMULATIONS

Our simulations have been done with $qN=0.01, 0.05,$ and 0.1 , all with $N=200$. For these values of qN , size effects with $N=200$ are negligible, as we comment in Sec. V C.

We define a characteristic height of the system as the height below which, on the average, 90% of the particles are.

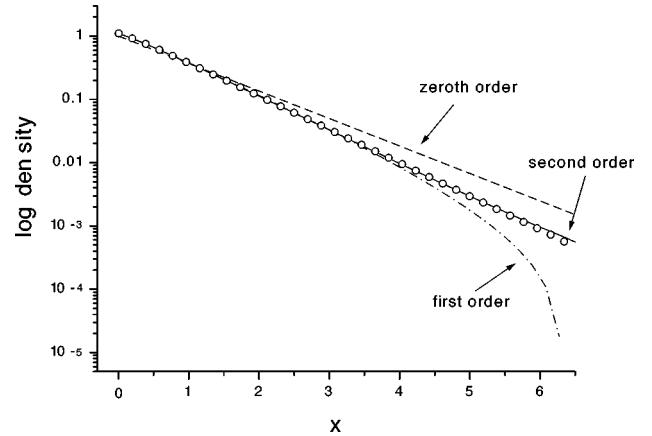


FIG. 3. The circles show in a logarithmic scale the density observed in a simulation of a system with $qN=0.1$ and $N=200$. The density is shown evaluated up to zeroth (dashed line), first (dot-dashed line), and second order (solid line). It can be seen that the prediction up to second order reproduces extraordinarily well the density far beyond the size ($X \leq 2$) of the system.

This characteristic height depends on qN but in the range we have worked it is roughly 2 (it varies from 2.7 at $qN=0$ to 1.65 at $qN=0.2$). In spite of this, the figures shown below cover a range up to $X=6$ where the density is three orders of magnitude smaller than near the base and the theory, up to second order, still gives good fits.

In our simulations—with an event-driven algorithm [18]—we have measured four local hydrodynamic fields: the number density $n(X)$, the adimensional local temperature $T(X)=\langle C^2/2 \rangle$, the adimensional heat flux $J_Q(X)=n(X)\langle C^3/2 \rangle$, and the fourth moment of the distribution. The first moment, $\langle C \rangle$, corresponds to the hydrodynamic velocity and it is zero both in theory and in the simulations.

Since the second-order correction was integrated numerically using a Monte Carlo algorithm, the results show, in some cases, noise coming from the integration procedure.

A. The density $n(X)$

The zeroth-order density $n_0(X)$ decreases exponentially, and since $qN \leq 0.1$, deviations from this behavior should be small. Dissipation prevents particles from reaching the heights they would reach in the conservative case and therefore the effective height of the system gets smaller and consequently the density tends to be higher near the base as shown in Fig. 3.

In Fig. 4 it is seen that both corrections grow from the base, and have a maximum slightly above it, therefore $n(X)$ is not necessarily monotonous. This means that when qN is large enough, the function $n(X)$ would have a maximum away from the base. We have numerically derived that $dn(X)/dX=0$ at $X=0$ when $qN \approx 0.5$. Hence for qN larger than this value, the density increases from $X=0$ and has a small maximum slightly over the base. It seems to us that this is the first manifestation of a phenomenon resembling a well known one: a liquid drop afloat a hot plate. Although this prediction is done from the low-density and quasielastic limit, we have measured this effect for simulations with $qN=1$.

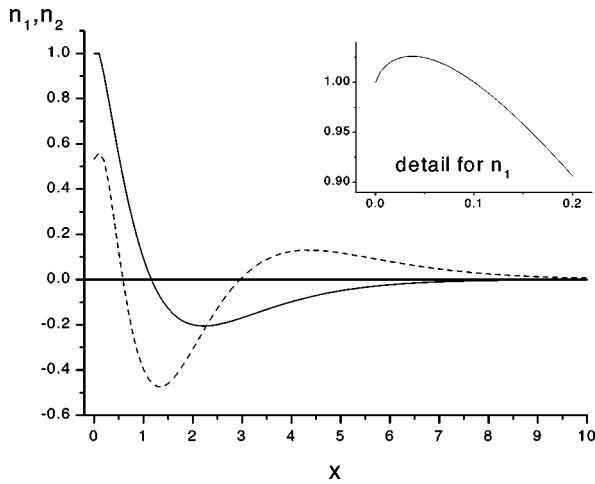


FIG. 4. The density is $n(X) = n_0(X) + qNn_1(X) + (qN)^2n_2(X)$. This figure shows n_1 (solid line) and n_2 (dashed line). The inset shows the maximum that n_1 has near $X=0$. The maximum of n_2 is seen in the main figure.

The effect of the corrections is seen in Fig. 3 for a system with $qN=0.1$ and $N=200$. When the second-order correction is included, the density is seen to be extremely well described. This figure also shows that the dissipative effects are overestimated using only the first-order distribution, while considering the second-order correction they are slightly underestimated.

B. The temperature $T(X)$

In Fig. 5 the temperature is shown for three values of qN . The zeroth-order temperature profile is the straight line $T = 1/4$ in all three cases. The effect of dissipation is to produce a $T(X)$ with negative gradient and this is already predicted by the negative first-order correction. The second-order correction, however, is positive all the way. In the

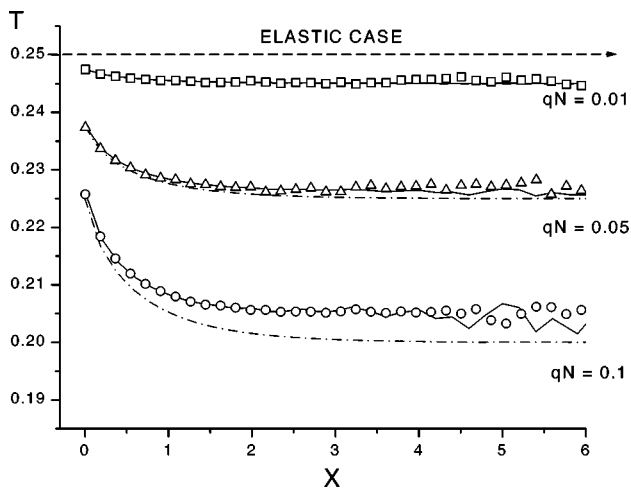


FIG. 5. If the system were perfectly elastic, the temperature (in adimensional units) would be uniform: $T = 1/4$. The figure shows for $qN=0.01$ (squares), $qN=0.05$ (triangles), and $qN=0.1$ (circles) that, because there is dissipation, the temperature decreases with height reaching an asymptotic value. The solid (dot-dashed) line is the predicted adimensional temperature up to second (first) order.

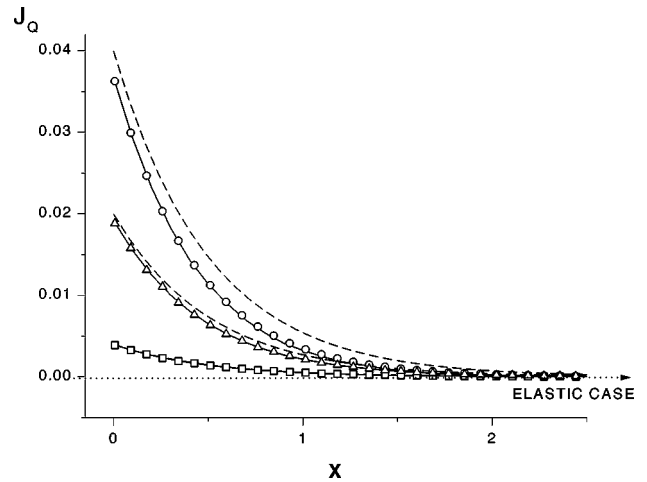


FIG. 6. The permanent energy influx through the base is dissipated in the “volume.” The figure shows the heat flux J_Q as a function of X for systems with $N=200$ and $qN=0.01$ (squares), $qN=0.05$ (triangles), and $qN=0.1$ (circles). The solid (dashed) lines give the respective heat fluxes evaluated up to second (first) order.

figure the temperature scale had to be amplified to be able to see the slight discrepancies between the predictions up to first and second order. In the less favorable case, namely $qN=0.1$, the first-order correction differs from the measured data by less than 5% while including the second-order corrections causes the fit to be excellent. Only our noisy estimate of the second-order correction prevented us from giving a good fit in the whole range. Figure 5 also shows that the temperature reaches an asymptotic value that our formalism predicts to be $T(X \sim \infty) \approx 1/4 - qN(1 - qN)/2$, which coincides with what we observe.

At $X=0$, the temperature of the system does not coincide with the imposed value $T_0 = 1/4$; there is a gap. In our case this *temperature slip* at the base is $\delta T \approx qN(1 - qN/2)/4$, which is the gap we observe. This wall thermal slip is a well known effect when the system has a temperature gradient [19,20] and it has been observed in real gases [21].

The heat flux seen in Fig. 6 is well described by the first-order correction when $qN=0.01$ but for larger values of qN the second-order correction gives an extraordinary prediction. From the figure it is seen that the heat flux is practically zero roughly at $X=2$ which is of the same order as the effective height of the system. Beyond that height particles almost have no collisions and the temperature is uniform.

V. FINAL COMMENTS

A. Overview of the results

It has been shown that a granular one-dimensional system of point particles —subjected to gravity and kept in a dilute time-independent state thanks to a steady energy input through a “hot base”— can be well described in the hydrodynamic limit by a Boltzmann equation. Adimensionalizing the problem allows us to transform away the parameters describing the acceleration of gravity and the temperature. In this sense one could say that in this *hydrodynamic limit* the system has, except for a scale factor, a universal behavior determined by qN .

An expansion in powers of qN of the distribution function has proved to yield a description of the system. In particular, it has been seen that the description up to second order in qN gives an excellent good fit of the hydrodynamics fields. The results regarding the moment $c_4 = \langle C^4 \rangle$ and the fits are equally good even though we do not report them. For $qN = 0.1$ a general feature is particularly evident, namely that the first-order correction overestimates the effects of dissipation. When the second-order correction is added there is an overall but small underestimation of dissipation.

Several results of the present paper should have their counterpart in two or three dimensions for very low density and close to the base. For example, the velocity distribution seen as a function of the velocity component perpendicular to the wall will, near the base, be anisotropic and its shape should be similar to that seen in Fig. 1. If the base is a hot wall and gravity \vec{g} points against the wall, the density will decay exponentially and the temperature will show a profile similar to those in Fig. 5. The theoretical framework will be somewhat different because the collisional term of Boltzmann's equation does not vanish in the elastic case (as it happens in 1D), but still, for regimes dominated by the boundary condition, like a Knudsen gas, one should expect that a perturbative solution obtained in much the same way as here should faithfully describe the behavior of the system. In dimensions higher than 1, the parameter that replaces our qN would probably be the parameter X defined in [3], $X = N(1-r)/n$, where r is the restitution coefficient, N is the total number of particles, and n is the average number of particles per layer. The quantity n , however, cannot be fixed a priori but it depends on the state of excitation of the system.

B. Physical picture and interpretation

Since in the elastic limit ($q=0$) our system of point particles is a gas of free particles passing through each other, the Hamiltonian is separable and therefore the Liouville distribution function is the simple product of one-particle distribution functions. Correlations are exactly zero. In this sense F_0 gives the exact solution of the statistical problem and, in particular, Boltzmann's equation is exact. This paper has built an approximate solution about F_0 when qN is small and correlations can be neglected.

Interpreting the system as one in which particles pass through each other losing some energy in the process—explained after Eq. (1)—it can be said that each particle starting from the base flies up and then comes down as if crossing a viscous fluid. This makes the average upward velocity larger than the average downward velocity. Correspondingly, then, the density of the up-moving particles is smaller than that for particles falling down.

Particles moving up have a vanishing most probable velocity, namely $F(C>0)$ is maximum at $C=0$, just like a Boltzmann distribution, while particles coming down are in principle accelerated, but the friction with the background (the rest of the particles) produces an effect similar to a ‘‘limit velocity’’ and $F(C<0)$ has a maximum away from the origin. These two characteristics can be appreciated, for example, in Fig. 2.

The abrupt change of behavior of the distribution at the base about $C=0$ can be understood because the particles near the base and going up are dominated by the thermal boundary condition; they have almost no information from the bulk and they are described by a distribution close to a Maxwellian, while the particles arriving at the base, carry the influence of all their passage through the bulk of the system. These two distributions meet at the origin of phase-space.

Moving away from the base the history of all particles tends to be comparable regardless of the sign of their velocity, and that is why the antisymmetric part of the distribution decays much faster than the symmetric part.

C. Effects of the size N of the system

To assess the conditions under which effects of the size N of the system appear, it is necessary to consider the adimensional version of Eq. (7) and the expanded distribution function (11). It is not difficult to see that the solution, expressed in terms of qN and N , takes the form

$$F = F_0 + qNF_1 + (qN)^2 \left(F_{21} + \frac{1}{N} F_{22} \right) + (qN)^3 \left(F_{31} + \frac{1}{N} F_{32} + \frac{1}{N^2} F_{33} \right) + \dots \quad (31)$$

We have evaluated these functions up to F_{22} and they are all of order 1.

The first appearance of an effect of the size of the system comes from $(qN)^2/NF_{22}$, namely if size effects enter at all, they do so as second-order effects. If, however, qN is small, the leading second-order term is already quite small and the size effects will be negligible unless N is small. Hence size effects become more apparent when qN is not too small and N is not too large.

On the contrary, to be absolutely sure that effects of the size of the system will not be appreciable *up to third order*, it is sufficient to require that $(qN)^2/N \ll (qN)^3$ (we are assuming that all the functions F_{ij} are of order 1), which implies that $N \gg 1/(qN)$.

The scale invariance that takes place when N is sufficiently large is exemplified in Fig. 7 for the case of the temperature. In this figure three systems with N equal to 20, 200, and 1000 are compared when $qN=0.1$ and $qN=0.01$.

While in the cases with $qN=0.01$ the temperatures for the three systems roughly coincide—except for some noise—in the cases with $qN=0.1$ the profile with $N=20$ shows higher temperature than those with $N=200$ and $N=1000$. The last two profiles fall one on top of the other (scale invariance).

D. A 1D gas of rods

If finite-size particles had been considered, some important aspects would remain the same because the system is one-dimensional. In fact, the evolution of two systems obeying the same collision rule (1), one composed of point particles and the other one composed of rods of size σ , can be put in a one-to-one correspondence. Call x_0 the positions of the lowest point-particle relative to the base, and successively x_1, x_2, \dots , the position of the following ones. Then

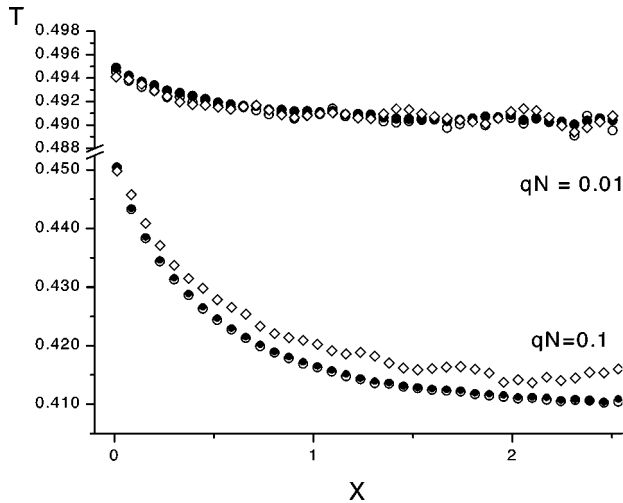


FIG. 7. The temperature profile, $T = \langle C^2/2 \rangle(X)$, observed in systems with $qN=0.01$ (upper set of points) and with $qN=0.1$ (lower set of points) and $N=20$ (rhombus), $N=200$ (solid circles), and $N=1000$ (open circles). For $qN=0.1$ the profiles with $N=200$ and $N=1000$ coincide because the size independent behavior has been reached while the points for $N=20$ show a higher temperature. For $qN=0.01$ even for $N=20$ the asymptotic behavior of the temperature has been reached because second-order corrections are too small.

the corresponding configuration for the rod system would be $z_k = k\sigma + x_k$. Since the collision rule is the same, it follows that starting from equivalent initial conditions $\{x_k, c_k\}$ and $\{z_k, c_k\}$ the two systems evolve to equivalent states at the

same pace. This one-to-one correspondence makes the Hamiltonian of the two systems equivalent, hence their associated Liouville equations can be transformed into one another. The difference becomes evident only when kinetic theory is reduced to that of a one-particle distribution function because the natural path to get a kinetic equation in the two cases is quite different. In one case it would naturally be a Boltzmann equation while in the other one it would be an Enskog equation. In other words, the collision terms appropriate to each case are not at all equivalent. Already in the perfectly elastic case the difference is evident as it has been analyzed in some detail in [8]. Let us use the interpretation given after Eq. (1), where the dynamics can be seen as if particles pass through each other. In the case of rods this implies that in every collision the particles involved make instantaneous jumps of length σ at infinite velocity. At the level of a kinetic theory for a one-particle distribution function this makes the collision term not trivial even in the elastic case, contrary to the case of point particles. One of the simpler effects of having rods is the appearance of a structured pair correlation function.

ACKNOWLEDGMENTS

We thank Dr. R. Soto for helpful discussions. We also thank J.M. Pasini and Professor D. Risso for their critical reading of the manuscript. This work has been partially financed by *Fondecyt* under Grant Nos. 197-0786 and 296-0021, and by the *Fundación Andes* under Grant No. C-12971. One of us (R.R.) thanks Becas Mutis from the Agencia Española de Cooperación Internacional for support.

-
- [1] H.M. Jaeger and S.R. Nagel, *Science* **255**, 1523 (1992); H.M. Jaeger, S.R. Nagel, and R.P. Behringer, *Phys. Today* **49** (4), 32 (1996); *Rev. Mod. Phys.* **68**, 1259 (1996).
- [2] J.A.C. Gallas, H.J. Herrmann, and S. Sokolowski, *Physica A* **189**, 437 (1992); Y. Zhang and C.S. Campbell, *J. Fluid Mech.* **237**, 541 (1992); S. Warr, J.M. Huntley, and G.T.H. Jacques, *Phys. Rev. E* **52**, 5583 (1995); N. Mujica and F. Melo, *Phys. Rev. Lett.* **80**, 5121 (1998).
- [3] S. Luding, H.J. Herrmann, and A. Blumen, *Phys. Rev. E* **50**, 3100 (1994).
- [4] A classic reference: P.K. Haff, *J. Fluid Mech.* **134**, 401 (1983). Recent works are B.C. Eu and H. Farhat, *Phys. Rev. E* **55**, 4187 (1997); J.W. Duffy, J.J. Brey, and A. Santos, *Physica A* **240**, 212 (1997); E.L. Grossman, T. Zhou, and E. Ben-Naim, *Phys. Rev. E* **55**, 4200 (1997).
- [5] K. Helal, T. Biben, and J.P. Hansen, *Physica A* **240**, 361 (1997).
- [6] Y. Du, H. Li, and L.P. Kadanoff, *Phys. Rev. Lett.* **74**, 1268 (1995).
- [7] E. L. Grossman and B. Roman, *Phys. Fluids* **8**, 12 (1996).
- [8] J. Ibsen, P. Cordero, and R. Tabensky, *J. Chem. Phys.* **107**, 5515 (1997).
- [9] E. Clément, S. Luding, A. Blumen, J. Rajchenbach, and J. Duran, *Int. J. Mod. Phys. B* **7**, 1807 (1993); S. Luding, E. Clément, A. Blumen, J. Rajchenbach, and J. Duran, *Phys. Rev. E* **49**, 1634 (1994).
- [10] S. McNamara and W.R. Young, *Phys. Fluids A* **4**, 496 (1992).
- [11] N. Sela and I. Goldhirsh, *Phys. Fluids* **7**, 507 (1995).
- [12] S. McNamara and W. R. Young, *Phys. Fluids A* **5**, 34 (1993).
- [13] I. Goldirsch and G. Zanetti, *Phys. Rev. Lett.* **70**, 1619 (1993).
- [14] R. Soto and P. Cordero, *Phys. Rev. E* **56**, 2851 (1997).
- [15] B. Bernu and R. Mazighi, *Phys. Rev. E* **50**, 4551 (1994).
- [16] S. Warr and J.M. Huntley, *Phys. Rev. E* **52**, 5596 (1995).
- [17] E.P. Gross, E. A. Jackson, and S. Ziering, *Ann. Phys. (N.Y.)* **1**, 141 (1957).
- [18] Event driven algorithms are an efficient tool to do molecular-dynamic simulations with hard particles: D.C. Rapaport, *J. Comput. Phys.* **34**, 184 (1980); M. Marín, D. Risso, and P. Cordero, *ibid.* **103**, 306 (1993).
- [19] A. Tenenbaum, G. Ciccotti, and R. Gallico, *Phys. Rev. A* **7**, 1690 (1993).
- [20] C. Trozzi and G. Ciccotti, *Phys. Rev. A* **29**, 916 (1984).
- [21] J.O. Hirschfelder, C.F. Curtiss, and R.B. Bird, *Molecular Theory of Gases and Liquids* (Wiley, New York, 1954).